Unified Inlet/Diffuser Design by an Inverse Method

G. J. Hokenson*
STD Research Corporation, Arcadia, Calif.
and
F. Y. Su†
Science Applications Inc., La Jolla, Calif.

The equations governing the two-dimensional, steady, inviscid flow of an incompressible fluid have been formulated in an inverse manner to obtain the resultant shape of semi-flush inlet/curved diffusers when the surface velocity distribution is specified. The results of calculations illustrating the effect of each of seven principal design variables on a nominal inlet configuration are presented. One of the configurations obtained was chosen for experimental testing to compare the on- and off-design performance of inlets generated by this procedure with that of inlets obtained by more conventional methods. General results and applications of this method are discussed.

Nomenclature

AR = area ratio, h_e/h_ℓ
d = vertical distance from inlet lip to ramp surface at $-\infty$, (Fig. 1)
DF = drop fraction, d/h_t
h_t = vertical height of ramp above inlet lip, (Fig. 1)
h = inlet height (Fig. 1)
IVR = inlet velocity ratio, U_ℓ/U_∞
K = inlet loss coefficient, $(P_{T_e}-P_{T_\infty})/q$ where: $q=q_\ell$ for $IVR>1$, $q=q_\infty$ for $IVR<1$.
L = ramp length (Fig. 1)
L_D = diffuser length (Fig. 1)
LVR = lip velocity ratio, U_{ϕ_r}/U_∞
ln = natural base logarithm
P_T = stagnation pressure
q = dynamic pressure
S_R = streamwise position, measured in inlet heights upstream from the lip, at which the ingested streamtube departs from a line which parallels the ramp (Fig. 1)
u = component of velocity in x direction
U = velocity vector magnitude, $(u^2+v^2)^{1/2}$
v = component of velocity in y direction
x = horizontal Cartesian coordinate normalized by L with origin at end of upstream uniform flow region
y = vertical Cartesian coordinate normalized by L with arbitrary origin
α = velocity vector angle, $\tan^{-1}(v/u)$
$\nabla^2_{\phi,\psi}$ = Laplacian operator in $\phi-\psi$ coordinates
δ = ϕ'/ϕ_e
$\Delta\phi$ = finite difference grid spacing in ϕ
$\Delta\psi$ = finite difference grid spacing in ψ
ϕ = velocity potential; Eq. (5) and (6)
ϕ' = $\phi-\phi_\ell$
ψ = stream function; Eq. (5) and (6)
τ = ingested streamtube length to height ratio, L/h_∞, (Fig. 1)
τ_D = diffuser length to height ratio, L_D/h_ℓ
θ = lip angle with respect to the vertical (Fig. 1)
ω = $\psi_{2,3}/\psi_4$

Subscripts

e = conditions at diffuser exit
i = streamline index
o = conditions at o (Fig. 2)
r = conditions at r (Fig. 2)
s = conditions at s (Fig. 2)
∞ = conditions along ramp surface infinitely far upstream
ℓ = conditions at inlet lip (Fig. 3)
1 = lowest bounding streamline in computation region (Fig. 2)
$2,3$ = dividing streamline which splits at the lip (Fig. 2)
4 = streamline which forms ramp and upper surface of diffuser (Fig. 2)

Introduction

INTAKE ducting in which an opening along a solid bounding surface to the flowfield is used to draw off fluid has been put to so many applications as to prohibit their explicit enumeration. Of prime importance among these applications are engine air inlets, auxiliary equipment inlets and boundary-layer suction slots, whether used in wind and water tunnels to "cleanse" the flow or to retard separation in a variety of adverse pressure gradient situations. For the majority of these inlet applications, a coupled diffuser is in evidence which allows the system to operate efficiently within the power constraints of the device which sustains the flow. Possibly equally as common is to have the diffuser curve

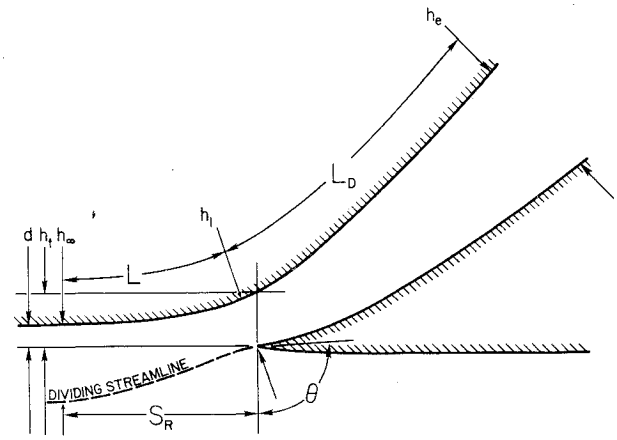

Fig. 1 Inlet configuration.

Received Jan. 5, 1976; revision received Aug. 12, 1976.
Index categories: Hydrodynamics; Subsonic and Transonic Flow.

*Group Manager and Senior Scientist, Physical Sciences Department. Formerly Supervisor and Senior Scientist, Waterjet Inlets, 2KSES Division, Rohr Industries, San Diego, Ca. Member AIAA.
†Scientist. Formerly Senior Scientist, Waterjet Inlets, 2KSES Division, Rohr Industries, San Diego, Ca. Member AIAA.

inboard from the flow surface along which the fluid is being drawn off. Initial experimental results obtained by the authors on inlets such as those shown in Fig. 1 indicate that the inlet geometry and flow conditions upstream of the lip, and to a finite but lesser extent on the downstream external lip, are strongly coupled to the pressure recovery and overall character of the flow inside the curved diffuser. This is not a particularly surprising fact, yet it is one which has received little intensive study. In general, the interaction effect of series/parallel hydrodynamically coupled components in a fluid system on the detailed flowfield is not yet understood. In engineering applications, established practice, guided by experience and some excellent classical experimental studies (e.g., Ref. 4-6), initiates the general design. Utilizing this procedure, many very efficient inlets have been developed after considerable empirical iteration on the design has been completed and which essentially compensates for these unknown interactions.

Dominant in the open literature with respect to their scope and intensity of experimental results are the publications of Mossman (e.g., Ref. 4) which, for inlet geometries of the general type investigated here, describe an optimum external pre-diffusion (indicated by an *IVR* less than one) for a given set of variations of a specific inlet configuration. These results have proved to be an invaluable guide in the development of inlets with relatively simple attached diffusers; however, the introduction of more complicated large-area-ratio, curved diffusers changes this picture significantly. The generation of curved diffuser shapes with relatively large expansions has been well documented in Ref. 3, supported by the analytical background developed in Ref. 1. The excellent experimental data obtained at Stanford[2,3] has served as a guide to the extent to which the boundary layers on each wall of a curved diffuser can support adverse pressure gradients, and indirectly the range of geometrical parameters which will result in an efficient pressure recovery device. There is little information available, however, which can serve as a guide to the unified design of an inlet/diffuser combination when large amounts of pre-diffusion, varying angle of incidence of the dividing streamline onto the inlet lip, and external lip geometry all interact with the internal diffuser area ratio, curvature, and length-to-height ratio. This gap in the information available in the open literature, coupled with the aforementioned experimental results, has directed the authors to look at some simple analytical tools for use in the design of such inlet systems and compare them experimentally to configurations which were designed without benefit of the analysis presented here.

With regard to the direct analysis of inlets and diffusers with a specified geometric configuration, the current state-of-the-art allows the full equations of motion with a sophisticated Reynolds stress tensor model to be applied to the duct. This approach is not, however, an efficient wall contour design technique and generally should be employed to expose the nonideal fluid flow phenomena associated with a family of optimum inlet shapes generated by an inverse method such as the one employed here. To the authors' knowledge, no such calculations utilizing the full equations of motion have been conducted on the generic type of inlet/diffusers considered here. However, some recent experimental studies carried out at NASA Lewis[7] evaluated annular Griffith diffusers whose design was guided by the results of Ref. 8. In this design procedure, the diffuser wall contour is obtained analytically whereas the details of the boundary-layer suction slot region are not emphasized. The results of Ref. 7 indicate a significant improvement in the performance of short annular diffusers with high suction flow rates. On the basis of the studies which are reported here, the detailed contours of the boundary-layer cutoff slot and associated ducting could possibly be optimized to improve diffuser recovery at a smaller suction flow rate. In support of this hypothesis, it has been the authors' experience that, while observing a hot wire anemometer signal in a boundary layer downstream of a suction slot, the entire character of the flow is extremely sensitive to the inlet *IVR*, lip position, and lip angle for a given overall suction flow rate.

Analytical Development

The design of a semiflush (i.e., $DF>0$) inlet/curved diffuser has been approached in an inverse manner to obtain the resulting physical shape of the bounding surfaces to the flowfield when the surface pressure or velocity distribution is specified. The equations governing the two-dimensional, incompressible, inviscid flow appropriate to this model of the flowfield have been solved over the entire region associated with the inlet, thus resulting in a unified shape which is totally consistent with any local change in the specified surface conditions. The calculation region includes the inlet ramp, curved diffuser, external lip, and the remote streamline which is the lower surface of the computation region shown in Fig. 2.

The governing equations of continuity and irrotationality expressed in spatial Cartesian coordinates and dimensional physical variables are

Continuity

$$\frac{\partial u}{\partial x}+\frac{\partial v}{\partial y}=0 \tag{1}$$

and

Irrotationality

$$\frac{\partial u}{\partial y}-\frac{\partial v}{\partial x}=0 \tag{2}$$

The dependent variables can be transformed from the x and y components of velocity to the velocity vector magnitude and angle via the following definitions

$$U=\sqrt{u^2+v^2} \tag{3}$$

and

$$\alpha=\tan^{-1}(v/u) \tag{4}$$

In addition, the independent variables can be transformed from a spatial Cartesian coordinate system to an orthogonal velocity potential-stream function system via the following transformations

$$\frac{\partial \phi}{\partial x}=\frac{\partial \psi}{\partial y}=u \tag{5}$$

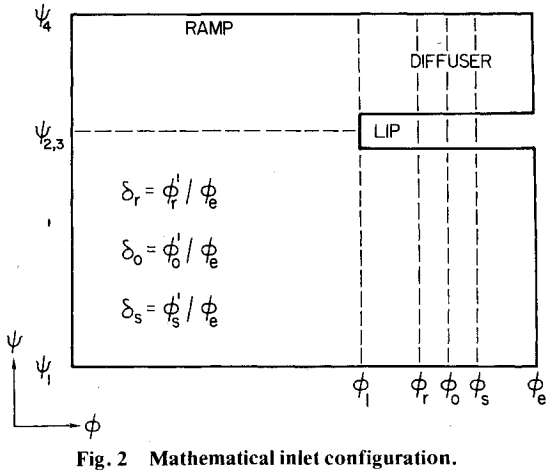

Fig. 2 Mathematical inlet configuration.

and

$$\frac{\partial\phi}{\partial y} = -\frac{\partial\psi}{\partial x} = v \tag{6}$$

Upon applying these transformations to the dependent and independent variables of Eqs. (1) and (2), the governing equations become

Continuity

$$\frac{\partial \ln U}{\partial\phi} + \frac{\partial\alpha}{\partial\psi} = 0 \tag{7}$$

and

Irrotationality

$$\frac{\partial \ln U}{\partial\psi} - \frac{\partial\alpha}{\partial\phi} = 0 \tag{8}$$

By cross differentiating and adding Eqs. (7) and (8), we obtain Laplace's equation for $\ln U$

$$\nabla^2_{\phi,\psi} \ln U = 0 \tag{9}$$

After imposing the appropriate boundary conditions on $\ln U$ in the ϕ-ψ plane, the entire field may be solved (in this paper using successive over-relaxation) for the distribution of $\ln U$ throughout a grid network appropriate to the inlet geometry as shown in Fig. 2. Once the distribution of $\ln U$ is known within the field of interest, the physical shape of the bounding surfaces may be obtained from the inverse transformation to Cartesian coordinates. Because of the orthogonality of the ϕ-ψ coordinate system, the inverse transformation can be formed from the following chain rule equations

$$dx = \frac{\partial x}{\partial\phi}\bigg|_\psi d\phi + \frac{\partial x}{\partial\psi}\bigg|_\phi d\psi \tag{10}$$

$$dy = \frac{\partial y}{\partial\phi}\bigg|_\psi d\phi + \frac{\partial y}{\partial\psi}\bigg|_\phi d\psi \tag{11}$$

The definitions of the independent variables given in Eqs. (5) and (6) allow us to write

$$d\phi = u\,dx + v\,dy \tag{12}$$

and

$$d\psi = -v\,dx + u\,dy \tag{13}$$

which can be solved for the appropriate derivatives in Eqs. (10) and (11) resulting in

$$dx = \frac{\cos\alpha}{U}\bigg|_\psi d\phi - \frac{\sin\alpha}{U}\bigg|_\phi d\psi \tag{14}$$

and

$$dy = \frac{\sin\alpha}{U}\bigg|_\psi d\phi + \frac{\cos\alpha}{U}\bigg|_\phi d\psi \tag{15}$$

These results may now be used to obtain the physical coordinates of each point on any streamline by integrating across ϕ along a constant ψ_i. The resulting equation for the x and y positions are

$$x_i(\phi) = x_i(o) + \int^\phi \left(\frac{\cos\alpha}{U}\right)_{\psi_i} d\phi \tag{16}$$

and

$$y_i(\phi) = y_i(o) + \int^\phi \left(\frac{\sin\alpha}{U}\right)_{\psi_i} d\phi \tag{17}$$

where the initial coordinates of each streamline are obtained by integrating Eqs. (14) and (15) along the line $\phi = 0$ from the plane of symmetry streamline to the streamline of interest as shown in the following equations

$$x_i(o) = -\int^{\psi_i} \left(\frac{\sin\alpha}{U}\right)_{\phi=0} d\psi \tag{18}$$

$$y_i(o) = \int^{\psi_i} \left(\frac{\cos\alpha}{U}\right)_{\phi=0} d\psi \tag{19}$$

It is now apparent that, to obtain the coordinates of each point on the streamlines of interest, the distribution of α along those streamlines must be obtained from the known lnU field. From the chain rule we can write

$$d\alpha = \frac{\partial\alpha}{\partial\phi}\bigg|_\psi d\phi + \frac{\partial\alpha}{\partial\psi}\bigg|_\phi d\psi \tag{20}$$

which, utilizing the conditions of continuity and irrotationality presented in Eqs. (7) and (8), may be rewritten

$$d\alpha = \frac{\partial \ln U}{\partial\psi}\bigg|_\psi d\phi - \frac{\partial \ln U}{\partial\phi}\bigg|_\phi d\psi \tag{21}$$

By integrating Eq. (21) along the particular streamlines ψ_i we may determine the distributions of α necessary to complete the integrations indicated by Eqs (16-19). Upon performing the indicated α integration along ψ_i we obtain

$$\alpha_i(\phi) = \alpha_i(o) + \int^\phi \left(\frac{\partial \ln U}{\partial\psi}\right)_{\psi_i} d\phi \tag{22}$$

Here again, the initial streamline angles are obtained by integrating in the ψ direction along $\phi = 0$ line from the plane of symmetry streamline to the streamline under consideration. This is done utilizing Eq. (21) and can be written

$$\alpha_i(o) = -\int^{\psi_i} \left(\frac{\partial \ln U}{\partial\phi}\right)_{\phi=0} d\psi \tag{23}$$

This completes the integrations which must be made utilizing the previously determined $\ln U$ field, resulting in the specification of the location of each point on the streamlines of interest in physical space.

Inasmuch as the input to the calculation is the surface velocity or pressure on the appropriate boundaries of the calculation region in the ϕ-ψ plane, appropriate distributions

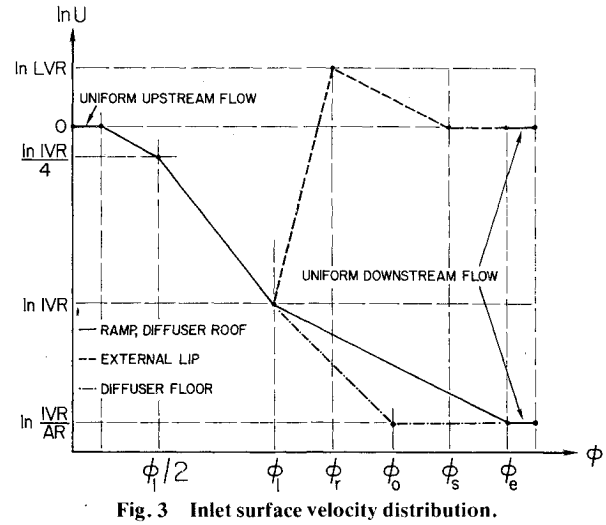

Fig. 3 Inlet surface velocity distribution.

must be selected. For simplicity and ease in manipulating their functional form numerically, velocity profiles of the form $U \sim e^{c\phi}$ were chosen to form various pieces of the distribution on the respective surfaces of the computation region and are depicted in Fig. 3. Reference 3 points out that one-dimensional flow considerations indicate that velocity distributions of this type are generated by straight wall two-dimensional channels if a one-segment exponential distribution is assumed to exist over the entire length of the channel. On all surfaces of the computation region not noted in Fig. 3, uniform flow may be specified.

The remote streamline was moved sufficiently far from the inlet so as to appear mathematically to be located at infinity. The boundary condition applied at this surface was that of zero normal derivative which forced this streamline to be a plane of symmetry between the inlet flowfield which was calculated and a fictitious mirror image inlet located equidistant beneath the plane of symmetry streamline. The theoretical desirability of having this plane of symmetry available is apparent in the utilization of Eqs. (18, 19, and 23) when we attempt to retrieve the physical shape of the bounding surfaces. In a practical sense, however, the plane of symmetry streamline was located sufficiently far from the inlet so as to have a negligible effect on the resulting inlet shapes, irrespective of the type of boundary condition (i.e., uniform flow or zero normal derivative) which was applied to it.

The effect of smoothing the assumed velocity distribution has been investigated; however, no significant changes in the general inlet shapes were found. Clearly, minor variations in the specific wall shapes ensued; however, no results were found which justified abandoning these straight-line profiles with the corresponding ease of manipulating the various parameters of interest. It is to be emphasized that the choice of this functional form for the boundary conditions is arbitrary and serves only as a reasonable distribution within which the effects of *IVR*, diffuser area ratio, diffuser and ramp length to streamtube height, diffuser curvature, and external lip shape on the resultant inlet configurations can be studied. There is an obvious restriction to the choice of this arbitrary distribution of surface conditions. It arises from the transformation itself which prohibits stagnation points in the flowfield. Therefore, the calculated shape of the inlet lip will necessarily be sharp. In actual practice, a parabolic noise will be faired in locally.

Discussion of the Results

The analysis which has been presented was programmed in double precision and coded in FORTRAN for execution on an IBM 370/168 computer. The computation grid was divided into a 200 $\Delta\phi \times 150\Delta\psi$ rectangular finite-difference mesh which was uniform in each direction. It was determined from numerical experimentation that an optimum position for the lip streamline occurred at a ψ value which allowed 25% of the total number of ψ lines to be located within the inlet streamtube. With the lip streamline located in this position, the solution (obtained through successive over-relaxation) relaxed to its final state in the fewest iterations and was the most accurate (as indicated by the final calculated area ratios of the inlet from its uniform upstream to its uniform downstream) at the maximum iteration limit as shown in Fig. 4. Fixing the lip at a particular ψ line forced $\Delta\psi$ to vary from case to case in order that various diffuser configurations might be calculated with different non-dimensional design parameters. Utilizing this uniform rectangular grid whose aspect ratio varied somewhat with the particular inlet being designed, computational times showed some variation. However, a general rule was that, with an over-relaxation parameter of 1.9, the inlet computation would arrive at an asymptotic solution within 400 to 600 iterations utilizing approximately 10 minutes of *CPU* time.

Once these preliminary setup constraints of the computational procedure were established, the parameters of the inlet surface velocity distributions were systematically varied. Of the parameters available, one was fixed as being a representative value for a desirable inlet shape. This was the quantity which reflected the number of uniform flow grid spaces which were placed upstream and downstream of the inlet. Extensive numerical experimentation established that 25 uniform flow grid spaces provided an adequate inlet shape in that all calculated surfaces were insensitive to further uniform flow additions.

The remaining inlet design parameters were varied in a consistent manner about a nominal inlet configuration to provide a comprehensive picture of how they influenced the resultant inlet shape. These parameters are: area ratio (*AR*), inlet velocity ratio (*IVR*), external lip velocity ratio (*LVR*), diffuser

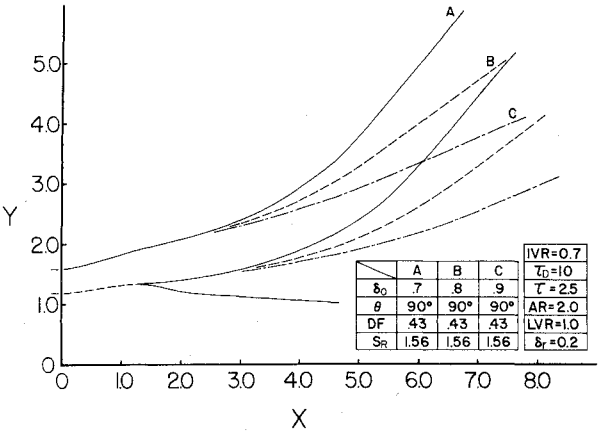

Fig. 5 Effect of δ_0 on inlet shape.

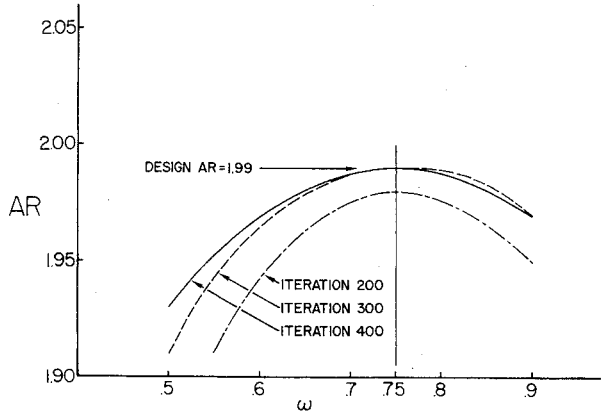

Fig. 4 Effect of lip streamline position on solution convergence.

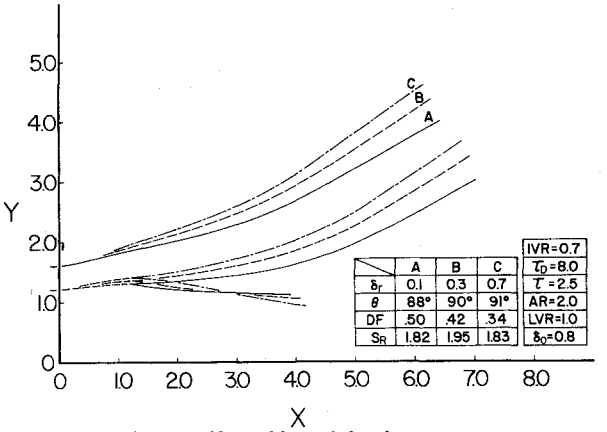

Fig. 6 Effect of δ_r on inlet shape.

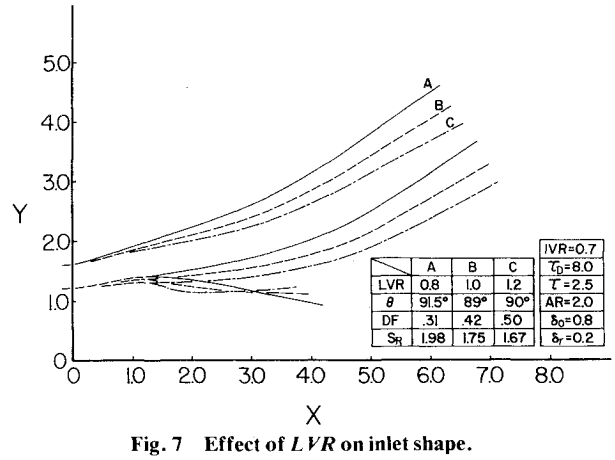

Fig. 7 Effect of LVR on inlet shape.

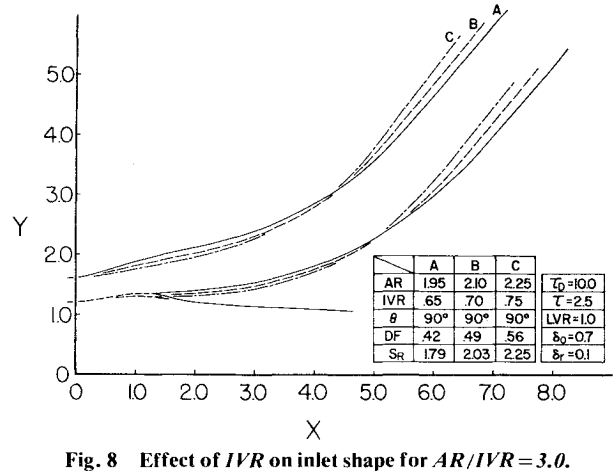

Fig. 8 Effect of IVR on inlet shape for $AR/IVR = 3.0$.

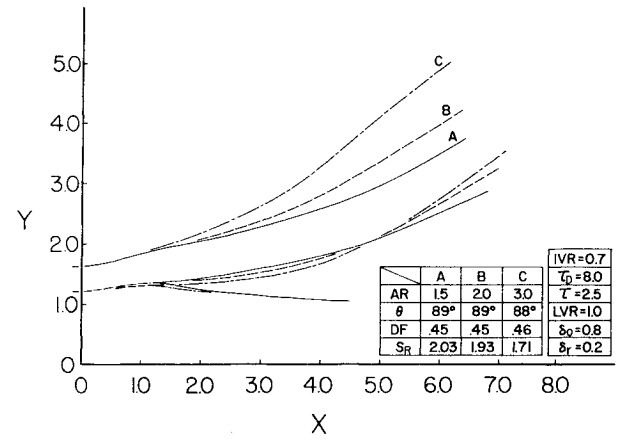

Fig. 9 Effect of AR on inlet shape.

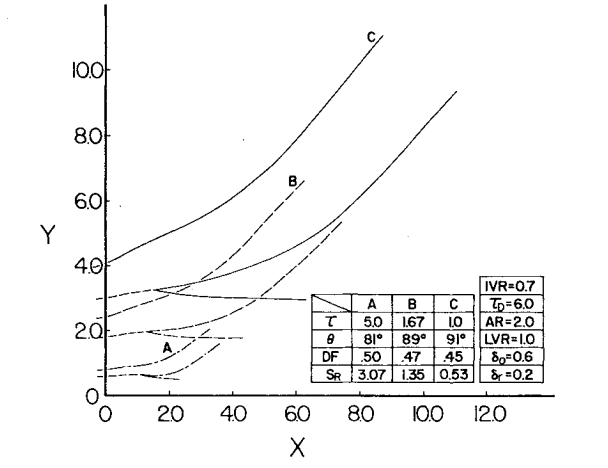

Fig. 10 Effect of τ on inlet shape.

lower surface velocity distribution factor (δ_o), external lip velocity distribution factor (δ_r), diffuser length to height ratio (τ_D), ramp length to streamtube height ratio (τ), and external lip velocity distribution factor (δ_s) which was held at the constant value of 1.0 after it was determined that LVR and δ_r exercised sufficient control over the external lip shape. The effect of these parameters on the surface velocity distribution is shown in Figs. 1 and 3. Apart from the basic sensitivity of the inlet shape to these input parameters, secondary inlet characteristics can also be obtained from the calculations. Those inlet characteristics which are an output of the analysis are drop fraction (DF), inlet lip angle (θ), and the ramp position (S_R) at which the ingested streamtube departs from a line which parallels the ramp, as shown in Fig. 1.

The resultant inlet configurations which are generated when each of the seven principal design variables are varied about a reference state are presented in Figs. 5–10. Although each of the design variables influence all parts of the final inlet shape, for the purpose of general discussion, their principal effects can be separated fairly clearly and general statements as to the characteristics of the inlets controlled by each can be formulated.

The effect of δ_o, which controls the diffuser lower surface velocity distribution as shown in Fig. 3, on the inlet shape is primarily the degree to which the diffuser exit curves inboard and directs the flow away from the freestream as shown in Fig. 5. Negligible changes in the lip angle, drop fraction, and ramp shape were observed. However, of primary importance are the relatively flat ramp and the thin lip which allows the flow to diffuse significantly prior to being turned; which are characteristic of all inlets presented here.

Control over the external lip shape is exercised primarily by the parameters δ_r and LVR whose influence on the velocity distribution is also shown in Fig. 3. The resultant shapes for various values of δ_r and LVR are shown in Figs. 6 and 7 where, apart from the lip shape (which can be changed from concave to convex by a small change in either variable), the principal effect is to lower the diffuser without significant change in the exit angle as the external lip flow acceleration is increased. Changes in the drop fraction are more sensitive to changes in LVR than they are to changes in δ_r, however the general characteristics of a flat ramp in the neighborhood of the inlet lip and a diffuser which attempts to separate turning and diffusion remain intact.

In order to expose the dependence of the inlet shape on IVR, the total diffusion (i.e., AR/IVR) was held constant at 3.0. The results presented in Fig. 8 illustrate two principal features of these inlets as IVR and AR are varied. The first effect which is worthy of note is the sensitivity of lip drop fraction to IVR, which was also observed on some calculations conducted for a fixed diffuser area ratio as both the IVR and total diffusion change. The second principal feature of the inlets with varying IVR is the rapid change in the characteristic shape of the external lip. The results in Fig. 8 indicate this quite clearly when comparing the lip shapes for $IVR = 0.65$ and 0.75. Because it obscured the figure, the lip for $IVR = 0.70$ was deleted. In the calculation of inlet shapes with a fixed diffuser area ratio, the effect of IVR on the external lip shape was even more pronounced than that shown in Fig. 8.

The effect of changing the diffuser area ratio at a constant IVR is shown in Fig. 9 where a fairly complex change of the diffuser exit angle and diffuser upper surface position are observed. The ramp, external lip, and diffuser lower surface are, however, relatively invariant with AR.

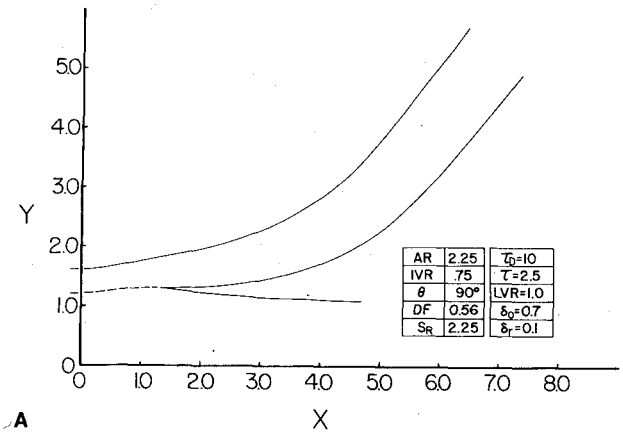

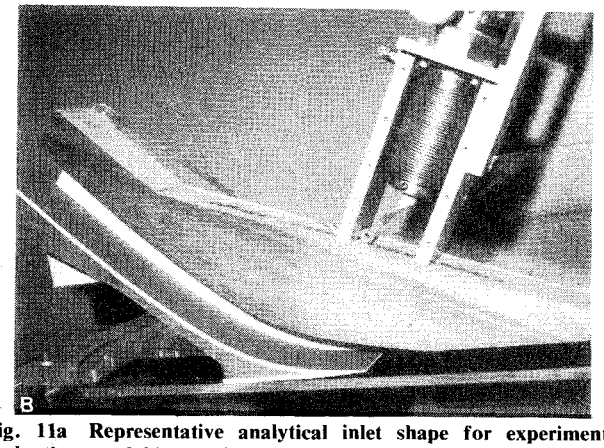

Fig. 11a Representative analytical inlet shape for experimental evaluation; and b) experimental model with sideplate and suction source removed.

Two design control variables whose effect is not shown explicitly on the velocity distributions in Fig. 3 are the diffuser length to inlet height ratio (τ_D) and the ramp streamtube length to height ratio (τ). These variables enter the analysis in the transformation from the assumed surface velocity distribution in physical space to the velocity distribution in ϕ and allow the characteristic ϕ values of Fig. 3 to be determined. The influence of an increasing τ_D on the inlet shape is to a very good approximation simply a stretching of the diffuser around the curvature determined by the diffuser turning parameter (δ_0). Some additional effects of secondary importance were slight changes in the lip shape and the extent of the parallel wall, uniform flow region at the diffuser exit.

The results for a varying τ are shown in Fig. 10 where the reference length used in the calculations (the length of the ramp to the point where $\phi=\phi_\ell$) is held constant and the overall inlet decreases in size as the height of the ingested streamtube is varied. The inlet contours presented in Fig. 10 indicate that both the lip angle and the departure point for the ramp streamtube from the ramp are strong functions of the parameter τ. These characteristics are even more apparent when the inlets are re-plotted for a constant inlet height with a varying ramp length.

In order to assess the utility of this design method in producing an inlet with adequate pressure recovery capability, a representative inlet configuration (shown in Fig. 11a and 11b) was selected for experimental evaluation. A small, two-dimensional indraft wind tunnel was built for this purpose. A centrifugal blower was utilized to draw room air through a 10:1 area ratio inlet contraction which contained a series of filters, flow straightening honeycomb and turbulence damping screens. Inlet/diffusers which were tested with the general configuration shown in Fig. 1 were then inserted into the upper surface of the channel. Through active control of

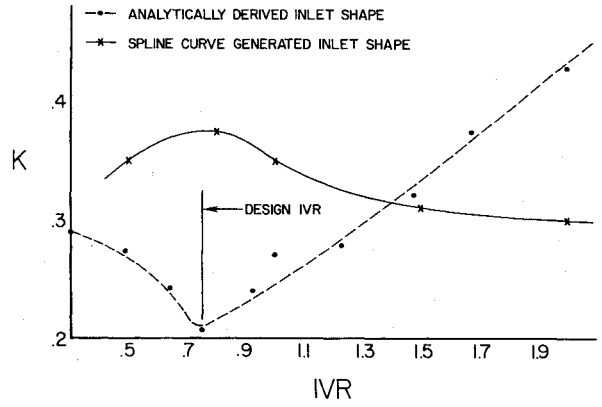

Fig. 12 Experimental inlet loss coefficients.

the surface roughness, the boundary layer approaching the inlet was adjusted to the desired thickness (approximately one-half the inlet height for the test data presented here). Attached to the exit of the inlet/diffuser was a rake of 13 total pressure probes located in the throat of a flow uniformizing venturi immediately downstream of the diffuser exit. Through utilization of the total and static pressure distribution data in the channel downstream of the diffuser exit, the pressure loss and flow rate through the duct were monitored. The magnitude of the flow rate through the inlet was controlled by means of valves located between the diffuser and a second centrifugal blower which was used to draw air from the mainstream flow within the wind tunnel and into the inlet.

The experimental results, presented in Fig. 12, also illustrate the overall inlet loss coefficient K vs IVR for an inlet designed by fitting spline curves through the desired inlet and exit positions of the diffuser and lip, which was tested in the same wind tunnel. The data are self-evident in justifying the ability of this method to generate high total pressure recovery inlets. Based on experience with a number of similar inlets in the course of this investigation, it is the authors' belief that lip angle, drop fraction, and diffuser turning/expansion distribution are the principal factors affecting the improved total pressure recovery supplied by inlets generated by the analysis presented here.

Conclusion

Inputting an arbitrary surface velocity or pressure distribution to the inlet design is a particularly desirable tack from several standpoints. First, from the point of view of retarding separation as long as possible it may be advantageous to specify the surface pressure distribution so as to avoid peaks in the pressure gradient or to match different experimentally observed pressure distributions which have been determined to delay separation on the ramp, diffuser upper surface, and diffuser lower surface. Second, for use in liquids, the ability to specify the surface pressure distribution is of considerable assistance in controlling the cavitation envelope of the inlet. Third, the consideration of imposing a specific pressure distribution on parts of the inlet to arrive at a favorable force and moment balance can be studied to determine the extent to which it interacts with the separation and cavitation performance. In this case, the unified aspect of this design procedure allows one to study directly the extent to which, for example, changes in the external lip lift force distorts the diffuser or inlet ramp geometry for a given ramp diffuser velocity distribution or forces a distorted ramp-diffuser velocity distribution for a given ramp-diffuser shape. Fourth, when a variable geometry inlet must be designed to operate efficiently at a variety of design points, the inverse method clearly illustrates which surfaces must be movable and in which general direction they must move to allow the inlet to be tuned to its optimum performance in that particular flowfield. Finally, the extent to which certain specified configurations impose unavoidable flow phenomena can be

studied by this method. An example of this involves the semi-flush nature of the inlets presented here. This inlet characteristic is a consequence of the fact that the analysis imposes a uniform flow at the inlet lip by having both the diffuser upper and lower surface velocity profiles originate at ln *IVR* as shown in Fig. 3. It is equally feasible to generate flush inlets by having the diffuser lower surface velocity distribution originate at values somewhat smaller than ln *IVR* and the diffuser upper surface velocity distribution at values somewhat larger than ln *IVR*, thus displacing the inlet lip downstream and more nearly flush. Therefore, we can infer that in a direct attack upon the inlet problem which specifies a flush-type inlet, it might be anticipated that non-uniform inlet velocity profiles could be generated with corresponding diffuser performance problems. This is only one example of the type of feature which a given geometry might impose on the flowfield, a result which becomes clear and casual in this inverse formulation.

Acknowledgment

The work presented here was conducted under contract to the U. S. Navy as a part of Contract Number N00024-74-C-0924.

References

[1]Stanitz, J. D., "Design of Two-Dimensional Channels with Prescribed Velocity Distributions Along the Channel Walls," *NACA Report*, 1115, 1953.

[2]Fox, R. W. and Kline, S. J., "Flow Regimes in Curved Subsonic Diffusers," *Journal of Basic Engineering, Transaction of ASME, Ser. D*, Vol. 84, 1962, pp. 303-316.

[3]Sagi, C. J., Johnston, J. P., and Kline, S. J., "The Design and Performance of Two-Dimensional Curved Subsonic Diffusers," *Report PD-9*, May 1965, Dept. of Mechanical Engineering.

[4]Mossman, E. A. and Randall, L. M., "An Experimental Investigation of the Design Variables for NACA Submerged Duct Entrances," *NACA RM A7130*, 1948.

[5]Hall, C. F. and Barclay, F. D., "An Experimental Investigation of NACA Submerged Inlets at High Subsonic Speeds," *NACA RM A8B16*, 1948.

[6]Sacks, A. H. and Spreiter, J. R., "Theoretical Investigation of Submerged Inlet at Low Speeds," *NACA TN2323*, 1951.

[7]Juhasz, A. J., "Effect of Wall Suction on Performance of Short Annular Diffuser at Inlet Mach Numbers Up to 0.5," *NASA TM X3302*, 1975.

[8]Yang, T., Hudson, W. G., and Nelson, C. D., "Design and Experimental Performance of Short Curved Wall diffusers with Axial Symmetry Utilizing Slot Suction," *NASA CR2209*, 1973.